Degradation in steam of 60 cm-long B4C control rods

Cristina Dominguez, Doris Drouan

Title: Degradation in steam of 60 cm-long B_4C control rods.

Authors: C. Dominguez, D. Drouan
Institut de Radioprotection et de Sûreté Nucléaire (IRSN), PSN-RES/SEREX/LE2M, St Paul-lez-Durance, 13115, France.
Tel.: +33 4 42 19 94 95.
Fax. : +33 4 42 19 91 62.
E-mail address: christina.dominguez@irsn.fr

ABSTRACT
In the framework of nuclear reactor core meltdown accident studies, the degradation of boron carbide control rod segments exposed to argon/steam atmospheres was investigated up to about 2000°C in IRSN laboratories. The sequence of the phenomena involved in the degradation has been found to take place as expected. Nevertheless, the ZrO_2 oxide layer formed on the outer surface of the guide tube was very protective, significantly delaying and limiting the guide tube failure and therefore the boron carbide pellet oxidation. Contrary to what was expected, the presence of the control rod decreases the hydrogen release instead of increasing it by additional oxidation of boron compounds. Boron contents up to 20 wt.% were measured in metallic mixtures formed during degradation. It was observed that these metallic melts are able to attack the surrounding fuel rods, which could have consequences on fuel degradation and fission product release kinetics during severe accidents.

KEYWORDS
Boron carbide, steam, degradation, control rod, nuclear reactor, severe accident.

1. Introduction

Boron carbide (B_4C) is a neutron absorber material used in many nuclear reactors worldwide to control the yield of the nuclear reaction. It is present as control rods in some of the pressurised water reactors (PWRs) and as control blades in boiling water reactors (BWRs). The behaviour of this type of material during core meltdown accident conditions is likely to play a significant role in the accident progression. This paper examines experimentally the behaviour of boron carbide in control rod geometries, in which the absorber is contained within stainless steel cladding, itself surrounded by a Zircaloy guide tube.

According to different authors [1-4], when the temperature rises in the reactor core during the initial accident phases, the Zircaloy guide tube is initially oxidised by steam, forming a zirconia (ZrO_2) scale on its external surface. Above temperatures of about 800°C, B_4C reacts with the stainless steel cladding, forming a mixture that melts at around 1200°C and reacts with the Zircaloy of the guide tube. This melt flows downwards inside the gap between B_4C pellets and the external ZrO_2 scale. Failure of the ZrO_2 external protective scale takes place beyond 1450°C and leaves the B_4C/steel/Zircaloy mixture flowing down towards the bottom of the core. In the absence of the cladding, the remaining B_4C pellets and the relocated mixtures will in turn be oxidised exothermically by the steam, leading to further increases in temperature and continued degradation of the control rod. These processes are currently poorly quantified and therefore need further investigation.

The BECARRE programme was carried out at the French “Institut de Radioprotection et de Sûreté Nucléaire” (IRSN) in the framework of the International Source Term Programme (ISTP) [5,6]. Its objectives were to improve understanding of the phenomena involved in the deterioration of the B_4C absorber materials and the determination of correlations for steam oxidation of the B_4C pellets and relocated mixtures. The BECARRE programme was divided into three parts. The first one, which was initiated within the COLOSS programme [7-9], concerned the steam oxidation of B_4C pellets [10]. The results have been already applied to improve computer codes that predict transient

progression in postulated reactor accidents [11-12]. The second part of the programme studied oxidation of B_4C-stainless steel mixtures and revealed that mixture oxidation rates were considerably lower than expected, even lower than those of solid B_4C pellets [13-14]. The last part of the BECARRE programme, presented in this paper, is closely related to the bundle tests QUENCH-07 and QUENCH-09 [15,16], to B_4C degradation tests performed within the COLOSS project [4,17] as well as to the Phebus FPT3 test [18]. It aimed at studying the partial degradation of control rods segments, the flowing down of the melts, the production of gases resulting from its oxidation (H_2, CO_2 and CO) and the probable interaction between the B_4C-steel-Zircaloy melts (which could have splashed out after the control rod failure) and the cladding of neighbouring fuel rods. Three degradation tests and a blank test carried out with a model rod instead of the boron carbide rod were performed.

2. Experimental set up and procedure

The experimental set up, presented in figure 1, includes:

- The INTERMEZZO furnace, an electrically-heated graphite vertical furnace equipped with 3 independent heating zones. This furnace is able to provide a thermal gradient along the rod axis.
- A vertical test section.
- A steam generator. Steam and argon flow rates can vary respectively between 0 and 16.7 g/min and between 1 and 20 l/min. Accuracies given by the manufacturer are $\pm$ 0.17 g/min and $\pm$ 0.2 l/min for steam and argon flow rates respectively.
- An INFICON™ CIS2 mass spectrometer to measure released gaseous products, except boric acids.
- A boric acid trap to remove boric acids formed during oxidation and to avoid their condensation inside the capillary tubes of the mass spectrometer.
- A condenser to remove unreacted steam.

The inlet and the outlet gas tubes up to condenser inlet, the boric acid trap and the spectrometer are heated to prevent steam condensation (presented in red in figure 1).

Tested specimens were a replica of a PWR 1300 MWe B_4C control rod centred inside a Zircaloy-4 guide tube. The control rod was composed of boron carbide pellets (ϕ= 7.47 mm, l=13.9 mm, ρ=1.79 g/cm^3) stacked into an AISI 304L stainless steel cladding (ϕ_{ext}=9.68 mm, ϕ_{int} = 7.72 mm). Total height of the B_4C column was 574 mm. The stainless steel cladding was He filled to 0.12 MPa in order to reveal cladding failure by helium detection in outlet gases. The Zircaloy guide tube (ϕ_{ext} = 12.45 mm, ϕ_{int} = 11.45 mm) was similar to the one used in the PHEBUS-FPT3 test [18]. In the last test (n°2), a ferrule (a Zircaloy-4 tube with ϕ_{ext} = 20.8 mm and ϕ_{int} = 19.2 mm) was added around the control rod to simulate the cladding of neighbouring fuel rods. The area of the ferrule radial section is equal to that of PWR fuel rod cladding exposed to melt projections from the control rod. The distance left between the guide tube and the ferrule was chosen in-between the distance of the two closest neighbouring cladding fuel rods in PHEBUS test geometry (between 1.819 and 7.038 mm) and close enough to the guide tube to favour melt projections and interaction with the Zircaloy ferrule.

Test conditions have been selected in order to be representative of severe accident conditions in a French PWR 1300 MWe reactor. It has been planned to limit B_4C degradation to 30% of the initial B_4C mass in order to keep enough intact material to detect the stopping level of the flowing molten mixtures [14]. As this degradation was not reached during the 1st test, experimental conditions were progressively made more severe in the following tests.

Experiments were carried out at atmospheric pressure and constant volume flow rate. Experimental conditions specific to each test are presented in table 1. Each test scenario followed this sequence: the upper and intermediate resistors were heated up to 900°C or 1000°C at 20K/min in an argon flow (9.5 Nl/min); the bottom resistor was heated at 20K/min up to 1000°C and stayed at this temperature during the entire test. After a temperature stabilisation period,

the argon flow was decreased to 1.5 Nl/min and steam was injected at 6 g/min during at least 2000s. This plateau is called the *pre-oxidation stage*. After the pre-oxidation stage, the upper and middle resistors were heated at 60K/min up to different temperatures according to the test and the resistor level and remained at these temperatures up to the end of the test. At the end of the test, the steam flow was switched off while the argon flow was increased to 9.5 Nl/min. Then, the furnace power was switched off. The stage lying between the end of the *pre-oxidation stage* and the end of the test is called the *degradation stage.*

In the first two tests (n°1 and n°1.2), steam injection was continuous from the beginning of the pre-oxidation stage to the end of the test. The thickness of ZrO_2 layer has been found to delay and limit control rod degradation. In the last test (n°2), pure Ar was injected from the end of the pre-oxidation stage until the internal test section temperature at upper resistor level achieves 1406°C (during 702 s). This way, ZrO_2 scale thickness is expected to be reduced to 30 µm when control rod degradation initiates. Then, the Ar flow was decreased to 1.5 Nl/min while steam was progressively re-injected at 12 g/min/min up to 6 g/min. Steam was gradually injected in order to limit the temperature escalation due to the Zircaloy ferrule oxidation.

A blank test identical to test n° 2 but carried out with two concentric Al_2O_3 tubes (ϕ_{ext}= 8 mm, ϕ_{int}= 5 mm and ϕ_{ext}= 4 mm, ϕ_{int}= 2 mm) instead of the B_4C control rod was also performed. This test permitted to quantify the H_2 release rate exclusively due to Zry oxidation and to measure the thickness of the ZrO_2 scales formed on the Zircaloy surfaces (ferrule and guide tube) in the absence of metallic melts (at high temperature, metallic melts dissolve the ZrO_2 scale).

Outlet gases (injected steam, and gases likely to be formed during oxidation, that is H_2, CO, CO_2 and CH_4) were measured on-line all over the test by mass spectrometry. The uncertainty of the outlet gas flow measurement has been evaluated to be lower than 14% of the measurement. Detection limits are $2 \cdot 10^{-3}$ mol/min for steam and $3 \cdot 10^{-4}$ mol/min for H_2, CH_4, CO and CO_2 except for test n°1, where detection limit is $1 \cdot 10^{-3}$ mol/min for both CO and CO_2.

Temperature of each furnace heating zone was regulated up to 1000°C with a retractable K-type thermocouple located at the middle height of the corresponding resistor and from 1220°C with a bi-chromatic optical pyrometer that points at the graphite resistor. Between 1000 and 1220°C, the furnace temperature was regulated by the weighted mean of both measurements. Inside the test section, temperatures were measured by means of 4 B-thermocouples located following the 4 points of the compass and at different heights, from top to bottom: 25 mm above and below the centre of the upper resistor, in the centre of the intermediate resistor and 8 mm below the lower resistor. These heights correspond respectively to 492, 442, 311 and 74 mm from the bottom of the control rod (at room temperature). Thermocouples were located inside thin alumina tubes to protect them against liquid metallic mixtures attack. Uncertainty of thermocouple measurements lies between 12°C at 700°C and 16°C at 1700°C.

Specimens which degraded during the first two tests (1 and 1.2) were photographed before being embedded in an epoxy resin. The last test specimen (n°2) was too fragile to be extracted from the test section. In consequence, it couldn't be photographed and was directly embedded in a resin. Embedded specimens were radiographed. Finally, specimens were sliced for microscopic and EPMA (Electron Probe Micro Analysis) examinations. To locate in height the radial sections and the measurement points of the thermocouples, we will use, in this document, their distance to the bottom of the guide tube. 2 mm is the uncertainty of the radial section position used for EPMA examinations (it takes into account uncertainties due to section location before slicing and due to material removed by slicing and polishing). Radiographs were performed by CEA (Commissariat à l'Energie Atomique et aux énergies alternatives) in the ROTONDE facility at Cadarache. This facility is equipped with a 160 kV X-ray generator and a numeric NTB X-ray detector [19-20].

Extensive post-test examinations were carried out with a LECA™ DMR microscope and a CAMECA™ SX-100 electron microprobe equipped with five WDS (Wavelength Dispersive Spectrometer), in order to identify the various chemical elements present at different elevations of the degraded rod. The standards used for quantitative chemical measurements were: Fe_2B (homemade standard also used in [13,21]) to quantify B and Fe, SiO_2 (CAMECA standard)

to quantify Si and pure element standards (from CAMECA) to quantify the other elements. Chemical quantitative analysis (15 kV, 50-100 nA) of analysed zones (300 µm x 300 µm) were performed by moving the sample by steps of 50 microns and sweeping at each step a 50 µm x 50 µm area by beam scanning (the analysed area was totally covered). Chemical composition, in wt.%, is the mean composition of the 49 individual areas. When the phases observed in an area have very different compositions that are not homogeneously distributed, the compositions measured in the 50 µm x 50 µm areas are scattered, leading to high standard deviations.
Carbon contents measured in this document are approximate because C was very difficult to quantify due to: beam contamination (even if an anti-contamination system was used, the measured C content increases with measuring time), epoxy resin (with high C content), that can increase the measured C-content when present in the vicinity of the analysed area and the high C content of the standard used compared to that of measured samples.
Zirconia thickness and B_4C pellet diameter measurements were performed with IM50 LEICA programme, version 1.2. The thickness of ZrO_2 scale formed on the surface of the Zircaloy components was measured on radial sections. On each radial section, four micrographs of external and internal guide tube and ferrule surfaces were taken following the 4 points of the compass. Ten regularly spaced measurements were obtained on each micrograph. The ZrO_2 thickness data are mean values of 40 measurements. Micrographs were obtained with magnifications between 25 and 200, depending on the ZrO_2 thickness, covering areas that vary from 360 x 268 to 2880 x 2141 μm^2. B_4C pellet diameters were calculated from radial sections as the diameter of the circle that has an area equal to the area of the B_4C pellet section.

3. Results

3.1. On-line measurements

Temperature profiles measured during the tests are presented in figure 2 together with the steam flow rate injected. As temperatures obtained during blank test are nearly identical to those obtained during test n°2, they are not presented in the figure. Relevant temperatures are summarised in table 2.
A technical problem caused a power cut off for 2 min 29 s during test 2, shown by a sudden temperature drop during the second heating ramp in figure 2. It can also be observed in this figure and in table 2 that test channel temperatures measured during the first two tests are sensibly lower than resistor temperatures (more than 100°C at the upper resistor level). A significant increase of the internal temperature was observed at steam injection during test 2. This increase is moderate at pre-oxidation stage and important at high temperature, causing the failure of internal thermocouples. As thermocouples are introduced at the top of the section, their failure doesn't mean that the temperature at the measurement point exceeded the maximum operating temperature of the thermocouple (1820°C). This is especially true for the lower thermocouple, located under the area heated only up to 1000°C. The other thermocouples show that temperature escalation and thermocouple failures are first observed at the intermediate resistor level and propagate downstream.
As thermocouples failed during test n°2, it was not possible to measure the maximum internal temperature. An order of magnitude of the maximum temperature reached was estimated by observing the appearance of the thermocouple protecting tubes after the test. The Al_2O_3 protecting tube reacted with the completely oxidised ferrule (ZrO_2) but without melting where they were not in contact. Consequently, the maximum temperature reached during test n°2 was comprised between those of the ZrO_2-Al_2O_3 eutectic (1866°C [22]) and the alumina melting point (2050°C [23]).
On-line gas flow measurements are presented in figure 3 together with the upper resistor temperature. Helium, released at cladding failure, was detected between 2 and 3 minutes before the end of the 2nd heating ramp during tests 1.1 and 1.2 and at the 2nd steam injection during test 2. It can be observed in table 2 that the detection of cladding failure takes place at similar temperatures, close to 1283-1312°C, consistently with the QUENCH experiment results [15-16]. Variable H_2 release was observed throughout steam injection: a small H_2 flow rate is observed during

pre-oxidation stage, whilst moderate and high H_2 flow rates are respectively measured during degradation stage in tests without (test n°1.1 and 1.2) and with ferrule (test n°2). In test n° 2, H_2 flow rate increases up to 0.25 mol/min while most steam is consumed (outlet steam is around 0.02 mol/min instead of the 0.33 mol/min injected).
It can be noticed in table 2 that the maximum H_2 release rate measured during test n°2 was respectively 10 and 5 times higher than those of tests n°1 and n° 1.2. In the three tests, this maximum is reached at the beginning of the high temperature plateau. At this moment, internal temperatures measured in tests n° 1.2 and n°2 differ significantly, even if both tests have the same 2nd plateau temperature: the internal highest temperatures during test n°1.2 are measured at the upper resistor level (T_{492} and T_{442}), while in test n° 2, the higher temperature is measured in the middle of the intermediate resistor (T_{311}).
H_2 and H_2O outlet flow rates measured during the blank test are also presented in figure 2. They are very close to those observed during test n° 2 but H_2 flow rate is slightly higher, mainly throughout the last 3 minutes.
CO and CO_2 were not detected during the first degradation test. (n° 1.1). During test 1.2, CO and CO_2 were released at similar low rates. Finally, during test n°2, CO was significantly released whereas only a small quantity of CO_2 was measured; a factor of 12 lower than that of test n° 1.2. Methane, that can be formed from B_4C oxidation gases (CO + H_2), has not been detected in any of the tests, consistently with the lack of methane observed in PHEBUS FPT3 [18] and QUENCH tests [16].
H_2 released by the oxidation of B_4C pellets can be roughly quantified considering that 4 moles of B are oxidized per mole of C and that H_2 is generated following the formulae:

$$C + H_2O \rightarrow CO + H_2 \quad (1)$$

$$C + 2\,H_2O \rightarrow CO_2 + 2\,H_2 \quad (2)$$

$$2\,B + 3\,H_2O \rightarrow B_2O_3 + 3\,H_2 \quad (3)$$

Results are presented in table 2 showing that oxidation of B_4C pellets generates about 40 % and 30 % of the total H_2 released respectively during tests n° 1.2 and n°2.

3.2. Post-test examinations

Figure 4 shows the appearance of the test specimens after degradation. Regarding test 2, the specimen was too fragile to be extracted from the test section and it was not photographed. On the left of the figure, the axial position of the furnace resistors (black strips) and of the thermocouple measurement points (white circles) are indicated. It can be noticed that the lower part of the specimens is not degraded and that all components can be distinguished except cladding and B_4C pellets that cannot be differentiated. Figure 4 also shows the location of radial sections presented in figure 5. The control rod and the ferrule of test n°2 broke before being resin-embedded and the lower part of both components moved 16 mm downwards. Since they did not fracture at the same height, the ferrule observed in section 263 was in fact 16 mm above this level during the test.
It can be observed in figures 4 and 5 that degradation of the rod and B_4C pellet consumption gradually increase with the distance from the bottom of the test section and thus with temperature. The degraded area extends following the chronological order of the tests.
In the intermediate part of the specimen, the gap between the guide tube and the cladding has been largely filled with metallic melts coming from higher levels of the test section. These metallic mixtures are produced by the eutectic reaction between B_4C pellets, stainless steel cladding and Zircaloy guide tube. Regions of relocated liquid materials are delimited by orange arrows in figure 4, falling as low as height 170 (test n°2).
High degradation can be observed at the upper resistor level. B_4C pellets, that can be clearly distinguished in radiographs inside the tube guide at this location, are moved off-centre, where the external surface of the guide tube is degraded and swollen. In the specimen from test n°2, ferrule distortion and swelling together with thermocouple melting can also be observed.

Radial sections of specimen n°2 (fig. 5) show that from section 315 upwards, the ferrule is completely oxidised. Moreover, in the upper sections, the guide tube is locally entirely consumed by metallic melts while the ferrule is severely damaged or broken at every contact point with the guide tube. In the same specimen, the two sections located at the upper resistor level show metallic melts corroding the inside of the ferrule: In section 433, the metallic melt is observed just where the guide tube interacts with the ferrule. In section 482, on the contrary, the metallic melt is observed even at regions far away and behind the guide tube; indicating that it comes from higher sections.
Evidence of liquid projections has also been observed after test n°1: Thermocouple protecting tubes that surround the rod have been corroded and show a purple colour. The same colour has been already observed on Al_2O_3 tubes used during the stainless steel–B_4C mixture tests [13]. Moreover, several small spherical metallic drops stuck to the outer surface of the guide tube and at the bottom of the test section have been observed, showing melt relocation outside the control rod.
Electron probe microanalyses have been performed on three radial sections of specimens 1.2 and 2, in order to characterise the solidified melts and to evaluate B and C contents. The analysed sections are located around the middle of the upper and intermediate resistors and at lower relocated mixtures. The mean chemical compositions of 300 µm x 300 µm areas were measured and are presented in table 3. Si and Mo were also measured but they were always lower than 0.2 wt.%. Measurement locations are presented in figure 5. The compositions of mixtures measured at the upper resistor level (sections 492 and 432 in rods 1.2 and 2 respectively) have up to 20 wt.% of B, and Zr contents vary between 9 and 69 wt.%. As SS-B_4C melt reacts with non-oxidised Zircaloy or ZrO_2 scale, it becomes enriched in Zr and impoverished in B, Cr and Fe. In sections located at the middle resistor level, the gap between the ZrO_2 scale formed on the external surface of the guide tube and B_4C pellet is almost completely filled with metallic melts where two different materials can be distinguished: *stainless steel-B_4C mixtures* (SS-B_4C) with B-contents around 9 wt.% and *stainless steel-B_4C-Zircaloy mixtures* (SS-B_4C-Zry), mainly in the zones close to the ZrO_2 scale, with B-contents between 6 and 14 wt.% and Zr contents between 41 % and 64 wt.%. SS-B_4C-Zry mixtures measured in specimen 2 are richer in B and poorer in Zr. An example of microstructures of both kinds of mixtures can be observed in figure 6.
The three initial components of the sample (guide tube, cladding and B_4C pellet) can be observed in sections around 220 mm level. At this level, gaps between these components are completely filled with metallic melts in rods 1.2 and 2. SS-B_4C mixture is observed between B_4C pellet and cladding in both rods and between the cladding and guide tube in rod n°2 (area 1 in sections 220 for test n°1.2 and 225 for test n°2 of fig. 5 and table 3). On the contrary, a SS-B_4C-Zry mixture is observed between the cladding and guide tube in rod n°1.2 (areas 2 and 3 in section 220) with B and Zr contents varying depending on the distance to the guide tube.
Zircaloy components are oxidised by steam, forming a zirconia (ZrO_2) scale on their external surfaces. The ZrO_2 scale is reduced in Ar atmosphere or in contact with steel-B_4C melts. It can be observed in figure 7 that the thickness of the ZrO_2 scale formed on the guide tube after the tests increases from the bottom to the mid-section of the rods where guide tube is completely oxidised (see sections 311-test n° 1.2 and 315-test n°2 in figure 5). Then, the ZrO_2 thickness decreases in the upper part of the rod. The higher ZrO_2 thickness is obtained after the blank test, the only test where the ZrO_2 scale is not corroded by metallic melts. The high standard deviation measured in rod n° 1.2 is due to the corrosion of the ZrO_2 scale by metallic melts that is radially very inhomogeneous. At the upper half part of the rod, only the guide tube of the first two tests withstands the metallic melt attack while it is almost totally consumed after the test 2, with the ferrule. The guide tube of the blank test was also completely attacked at the upper part. In absence of metallic melts, it was consumed at high temperature by the eutectic reaction with the Al_2O_3 of the model rod.
Figure 7 also shows the diameter of the B_4C pellets after the 3 degradation tests. It can be observed in this figure that the pellet consumption increases as test conditions become more severe, that is, following chronological order. After tests n° 1.2 and n°2, the diameter of B_4C pellets is similar except between levels 311 and 492 (between the middle of

the intermediate resistor and 25 mm above the middle of the upper resistor), where it is notably lower after test n°2, consistent with the higher degradation of the rod after this test.

5. DISCUSSION

The degradation of B_4C control rods, 60 cm long, has been studied under conditions representative of a severe accident in a PWR. To discriminate between the effects of Zircaloy and of boron carbide, a blank test was carried out with two alumina tubes instead of the B_4C control rod (following the same scenario of one of the degradation tests: test n°2).

When the temperature rises during the initial accident phases, the Zircaloy guide tube is initially oxidised by steam, forming a zirconia (ZrO_2) scale on its external surface. B_4C reacts with the stainless steel cladding and the Zircaloy of the guide tube forming a liquid mixture that flows towards the bottom of the core. After the failure of the ZrO_2 external protective scale, the remaining B_4C pellets and the relocated mixtures will in turn be oxidised by the steam. H_2 produced by the oxidation of these materials was observed in all tests throughout steam injection, but the H_2 flow rate measured in the blank test is slightly higher than in test n°2. This difference cannot be attributed to the temperature drop caused by the power cut-off observed during test n°2 because it occurred before steam injection. Only Zircaloy (of the guide tube and the ferrule) can be oxidized in the blank test. Consequently, the H_2 released during test n°2 is mainly produced by Zircaloy oxidation. It has been observed in figure 7 that the higher ZrO_2 thickness is obtained after the blank test, the only test where the ZrO_2 scale is not corroded by metallic melts. Furthermore, the upper half of the guide tube is almost totally consumed by metallic melts attack after the test n°2. As a result, the reason for the lower flow rate observed in test n°2 can be the capture of Zr by the metallic melts during test n°2. Thus, less Zr was available to be oxidized by steam and consequently less H_2 was released.

Steinbrûck et al. measured a lower quantity of H_2 in a test without boron carbide rod (QUENCH-08) than in a test with the absorber rod (QUENCH-07) [16]. These results, in contrast to BECARRE results, can be explained taking into account the differences between conduct of the tests. In the QUENCH tests, a temperature plateau at 1450°C is maintained after the failure of both control rod and guide tube and before the last heat-up phase. During this temperature plateau, oxidation of cladding, B_4C and relocated products take place under stationary conditions. In the BECARRE tests, the oxidation plateau takes place at temperatures about 300°C below the temperature of control rod failure. In this way, only the cladding is oxidised forming a zirconia protective scale. Then, temperature is increased under Ar, so the eutectic melts that forms inside the Zircaloy guide tube, have more time to react with the non-oxidised Zircaloy before the failure of the remaining guide tube at around 1550°C and the consequent B_4C oxidation.

High steam consumption was observed during test n°2, suggesting that steam starvation has taken place locally, as observed in the PHEBUS FPT3 test. The ferrule, which is not present in previous BECARRE tests, supplies a quantity of Zircaloy close to 3 times that of the guide tube. Zircaloy oxidation produces a large amount of heat. The heat generated by the oxidation of the ferrule increases significantly the internal temperature and thus accelerates the oxidation reaction. Consequently, the oxidation of the Zircaloy consumes a high quantity of steam. As steam is injected at the bottom of the test section, it is practically all consumed before reaching the upper resistor level. As a result, an internal temperature escalation is first observed at the intermediate resistor level and later at upper level, when the Zircaloy at the intermediate level is almost completely oxidized and allows steam to go upwards. Even if test n°2 is the one which has the shortest degradation period (about five and two times shorter that those of test n° 1.2 and n°1 respectively), the total H_2 quantity measured is respectively 2 and 6 times higher, due to oxidation of the Zircaloy ferrule and to the resulting higher temperatures.

The reducing atmosphere due to steam starvation is responsible for the high CO/CO_2 ratio observed during test n°2. C-gases could come from oxidation of B_4C pellets or from oxidation of C contained in the liquid mixtures formed during control rod degradation. However, B_4C-containing liquid mixtures relocate downwards (at low temperatures) and only

very small quantities of C oxides are released during oxidation of B_4C-containing liquid mixtures compared to B_4C pellets [13]. Consequently, CO and CO_2 releases mainly come from B_4C pellet oxidation.
In the ASTEC severe accident code, guide tube rupture is supposed to happen instantaneously after the failure of the cladding. Experimentally, cladding failure was detected when internal temperatures slightly exceeded 1300°C. Nevertheless, even if the temperature at which cladding failure was detected coincide with ASTEC expected temperature (1340 °C in [14]), the guide tube dislocation (associated to the release of significant quantities of C-oxides) did not occur at that time. No guide tube rupture was observed during test n°1 but only during subsequent tests. During test n°1.2, this rupture happened at 1657°C, a higher temperature than those obtained during COLOSS 10 cm-experiments (1375-1580°C in [4,17]). The thickness of the ZrO_2 scale during the second heating ramp (at the beginning of degradation) was reduced in the last test, leading to a decrease of about 100°C of the guide tube rupture temperature compared with test n° 1.2.

6. SUMMARY AND CONCLUSIONS

Three B_4C control rods, 60 cm long, have been degraded under conditions representative of a severe accident in a PWR. It was planned to reach a degradation of about 30 wt.% of the initial B_4C pellets by eutectic formation with stainless steel and oxidation reactions, after the guide tube dislocation [14]. This objective could not be reached during the first two tests due to both the protective thick ZrO_2 scale developed at the guide tube surface during the second heating ramp and the low temperature levels reached. To decrease the thickness of the ZrO_2 layer, the parameters of the third test have been modified: a large proportion of the second heating ramp has been performed under argon instead of steam atmosphere to reach a 30 µm scale at the time of the expected control rod degradation. Finally, the expected degradation has been achieved in the third test, revealing the importance of the protective effect of the zirconia layer (not considered in ASTEC) in moderate degradation scenarios.
After the cladding failure, the H_2 release rate increases up to a maximum that coincides with the beginning of the high temperature plateau. The H_2 release is mainly produced by Zircaloy oxidation. In the presence of a boron carbide rod, a decrease of H_2 release is observed caused by the dissolution of Zircaloy by SS-B_4C melts which limits the B_4C and B_4C-SS melt oxidation.
It is important to note that the rod surroundings, represented in the last test by a Zircaloy ferrule, have an important role in the degradation of B_4C rods. The oxidation of the ferrule notably increases the temperature and induces the release of high quantities of H_2. The higher temperature promotes a higher degradation, that is, a higher consumption of B_4C pellets and the formation of high quantities of metallic melts. The formation of high quantities of H_2 and the consumption of the majority of the steam result in local steam starvation that propagates upwards, and the temporary reducing atmosphere promotes the formation of CO instead of CO_2.
The composition of metallic mixtures formed during degradation is varied. Stainless steel-B_4C mixtures have B-contents around 9 wt.% while stainless steel-B_4C-Zircaloy mixtures reach B-contents between 6 and 20 wt.%. Metallic melts are mainly contained by the zirconia scale formed on the external surface of the guide tube but they also reach and attack the surrounding ferrule. So, during a severe accident, metallic melts can contribute to the degradation of the cladding of surrounding fuel rods and therefore could have consequences on fuel degradation and hence on fission product release kinetics.
A review and code interpretation of the whole BECARRE programme is presented in a companion paper [14].
BECARRE test results have been extensively used to improve the B_4C degradation modelling implemented in the ASTEC severe accident code [11,14]. Results contributed also to the study of the boron behaviour in the primary circuit of water reactors under severe accident conditions [24].

Acknowledgements

The partners of the International Source Term Programme, conducted by IRSN, are acknowledged for their support and contributions: CEA, EDF, EC, Suez/Tractebel (Belgium), PSI (Switzerland), AECL (Canada) and USNRC (USA). The authors are very grateful to G. Montigny for their collaboration in post-test examinations, to J. L. Pettier, N. Estre and D. Eck from CEA for radiographs, to O. De Luze for his helpful comments on the experimental results and to Ph. March, B. Teisseire and T. Haste for their careful reviews of this paper.

References

[1] P. Hofmann, S. J. L. Hagen, G. Schanz, A. Skokan, Reactor core materials interactions at very high temperatures, Nucl. Technol. 87 (1989) 146-186.

[2] P. Hofmann, M. Markiewicz, J. L. Spino, Reaction behaviour of B_4C absorber material with stainless steel and Zircaloy in severe light water reactor accidents, Nucl. Technol. 90 (1990) 226-244.

[3] L. Belovsky, V. Vrtílková, M. Valach, R. Gonzalez, Chemical interactions in B_4C-filled control rod segments above 1000°C under transient conditions, in: 5th International Conference on Nuclear Engineering ICONE5, Paper 2148, Nice, France, May 26–29, 1997.

[4] M. Steinbrück , Degradation and oxidation of B_4C Control Rod Segments at High Temperatures, J. of Nucl. Mater. 400 (2010) 138-150.

[5] B. Clement, R. Zeyen, The PHEBUS Fission Product and Source Term International Programme, International Conference Nuclear Energy for New Europe, Bled, Slovenia (2005). http://www.djs.si/proc/bled2005/htm/tocFrameSet.htm.

[6] B. Clement, B. Simondi-Teisseire, International Source Term Programme: Recent Results and Prospects, CSARP Meeting, Bethesda, September 16th-18th (2008).

[7] B. Adroguer et al., Core loss during a severe accident (COLOSS), Nucl. Eng. and Des. 235 (2005) 173-198.

[8] B. Adroguer et al., Core loss during a severe accident (COLOSS), Nucl. Eng. and Des. 221 (2003) 55-76.

[9] M. Steinbrück, Oxidation of boron carbide at high temperatures, J. of Nucl. Mater. 336 (2005) 185-193.

[10] C. Dominguez, N. Cocuaud, D. Drouan, A. Constant, D. Jacquemain, Investigation on boron carbide oxidation for nuclear reactor safety. Experiments in highly oxidising conditions, J. of Nucl. Mater. 374 (2008), 473-481.

[11] N. Seiler, O. Marchand, G. Repetto, S. Ederli, Investigation on boron carbide oxidation for nuclear reactor safety. General Modelling for ICARE/CATHARE code applications, Nucl. Eng. and Des. 238 (2008) 820-836.

[12] H. Steiner, Modeling of boron carbide oxidation in steam, J. of Nucl. Mater. 345 (2005) 75-83.

[13] C. Dominguez, Steam oxidation of boron carbide-stainless steel liquid mixtures, J. of Nucl. Mater. 427 (2012) 140-151.

[14] O. De Luze, Degradation and oxidation of control carbide segments at high temperatures. A review and code interpretation of the BECARRE program, Nucl. Eng. and Des. 259 (2013) 150-165.

[15] L. Sepold et al., Results of the QUENCH-09 experiment compared to QUENCH-07 with incorporation of B4C absorber, Nucl. Tecnol. 154 (2006) 107-116.

[16] M. Steinbrück, M. Groβe, L. Sepold, J. Stuckert, Synopsis and outcome of the QUENCH experimental program, Nucl. Eng. and Des. 240 (2010) 1714-1727.

[17] M. Steinbrück, A. Meier, E. Nold, U. Stegmaier, Degradation and oxidation of B_4C Control Rod Segments at High Temperatures. Report FZKA-6980, Forschungszentrum Karlsruhe, May 2004.

[18] F. Payot et al., PHEBUS FPT3 Final report, IRSN report Phébus PF IP/11/589, July 2011.

[19] J. L. Pettier, N. Estre, D. Eck, Compte-rendu d'examens par Imagerie X : essais BECARRE 1 et 1.2, CEA internal report DEN/DTN/SMTM/LMN/NT/2010/015ind.0, April 2010.

[20] N. Estre, J. L. Pettier, Compte rendu d'imaginerie X sur crayon dégradé BECARRE n°2, CEA internal report DEN/DTN/SMTM/LMN/ 2010 DO 133, 2010.

[21] S. Sao Joao, C. Duriez, C. Dominguez, D. Jacquemain, Light elements microanalysis of steel/B_4C melts for nuclear power plants accident studies, Microchim Acta, 162, (2008), 343-348.
[22] D. A. Jerebtsov, G. G. Mikhailov and S. V. Sverdina, Phase diagram of the system: Al_2O_3-ZrO_2, Ceram. Int., 26 (2000) 821-823.
[23] S. J. Schneider Jr. (ed.), Engineered Materials Handbook vol.4: Ceramics and Glasses, ASM International, Materials Park, Ohio, USA, 1991.
[24] T. Haste et al., Study of boron behaviour in the primary circuit of water reactors under severe accident conditions: A comparison of Phebus FPT3 results with other recent integral and separate-effects data, Nucl. Eng. and Des. 246 (2012) 147-156.

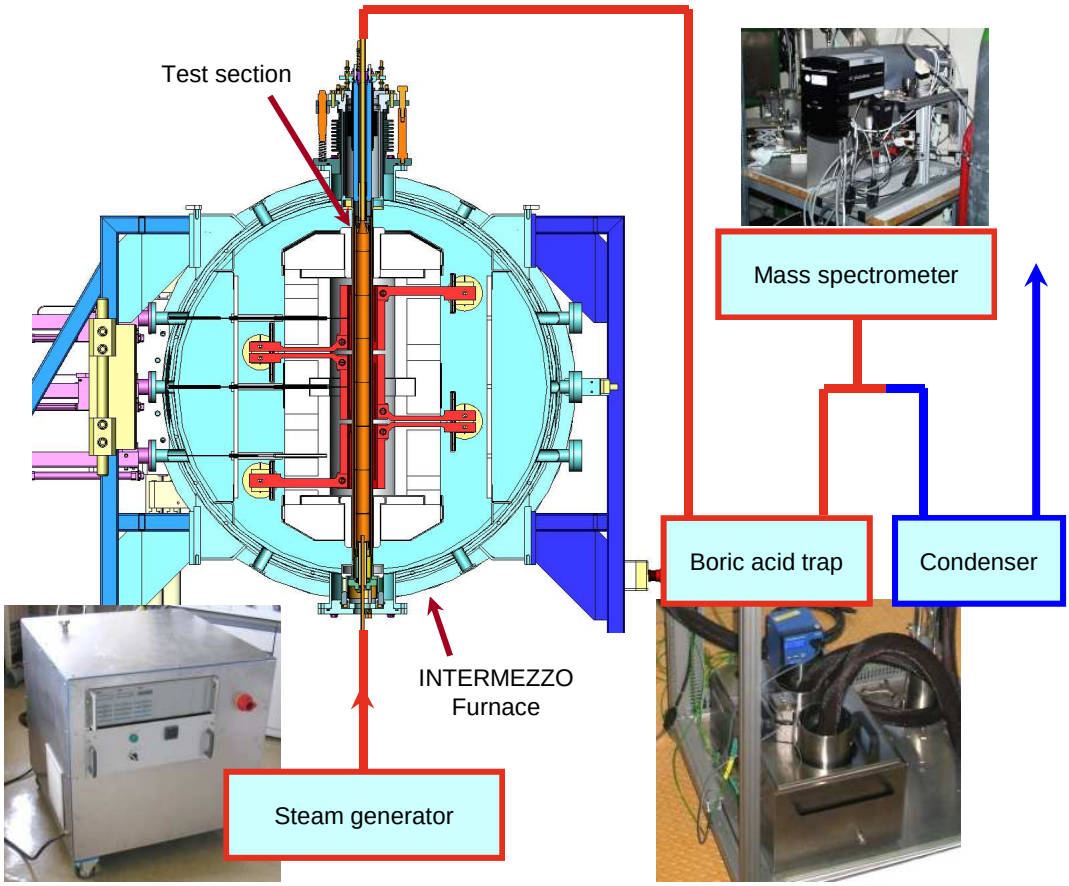

Figure 1 : Experimental facility

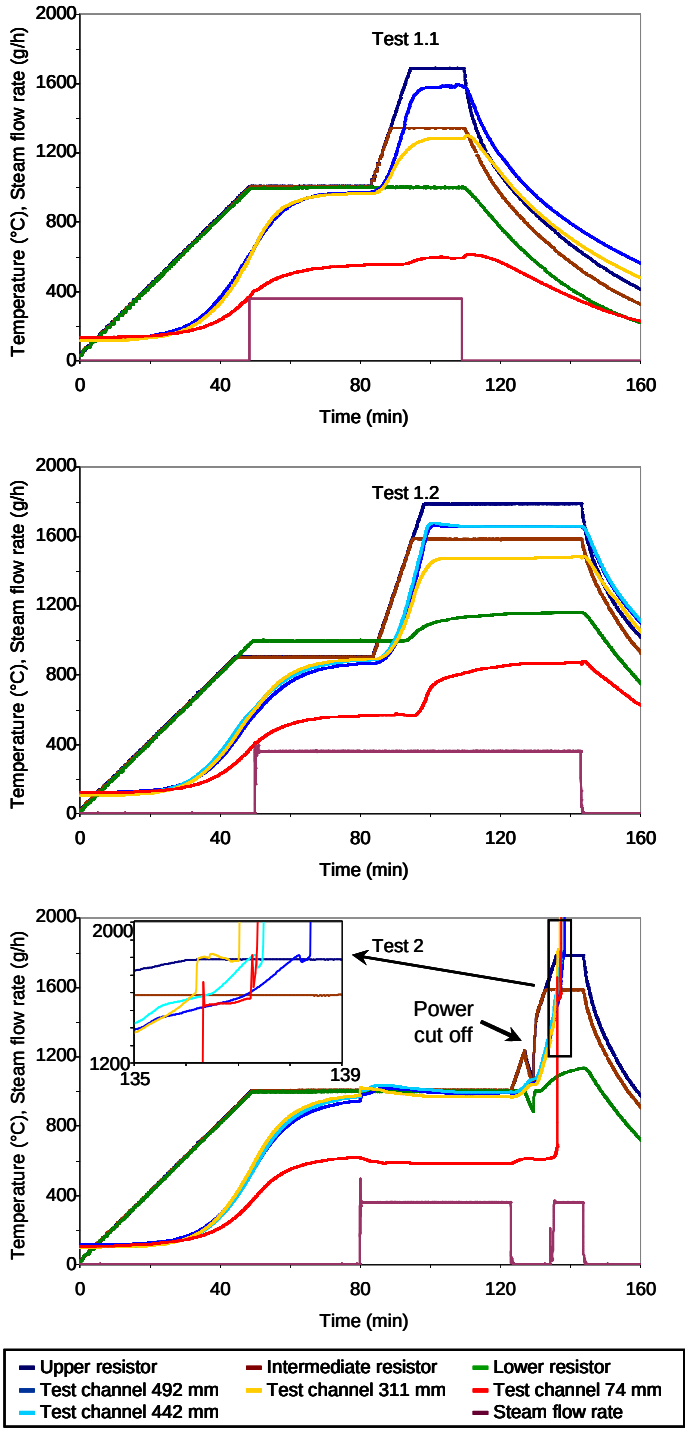

Figure 2: Temperature measurements.

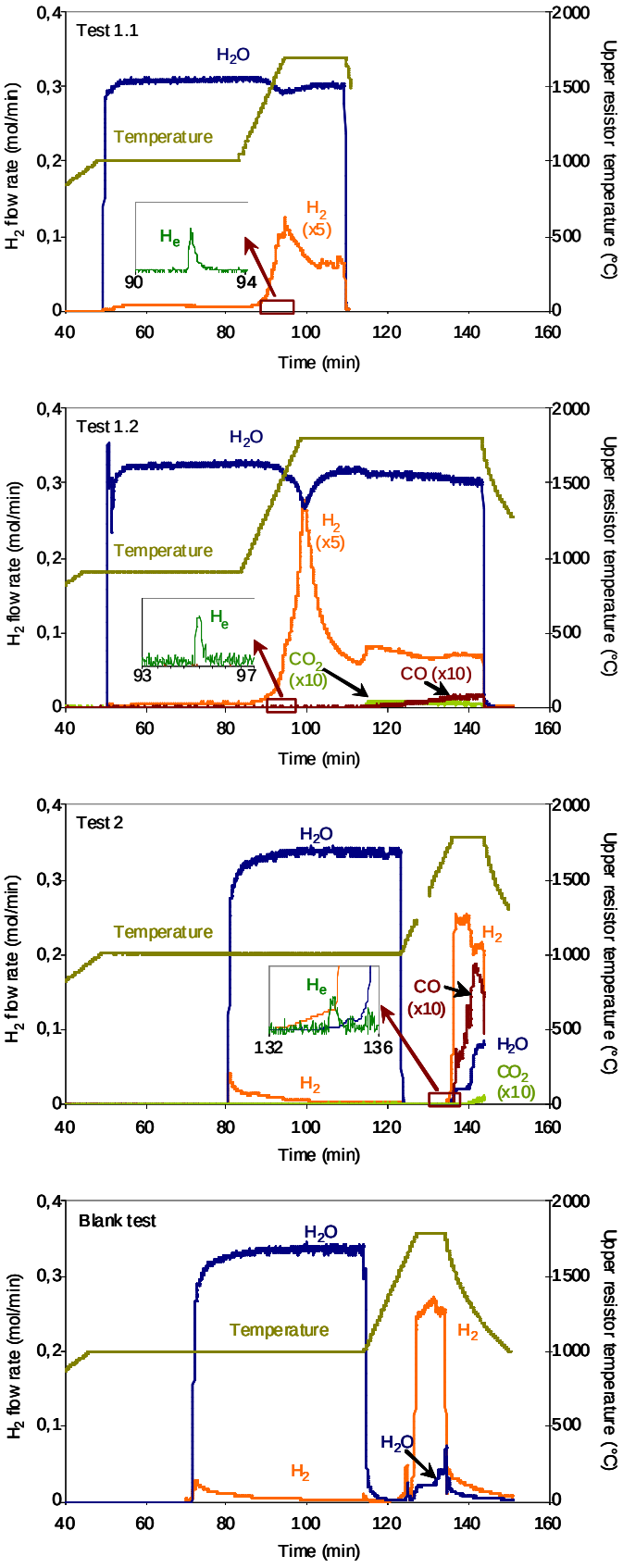

Figure 3: Outlet gas flow measurements.

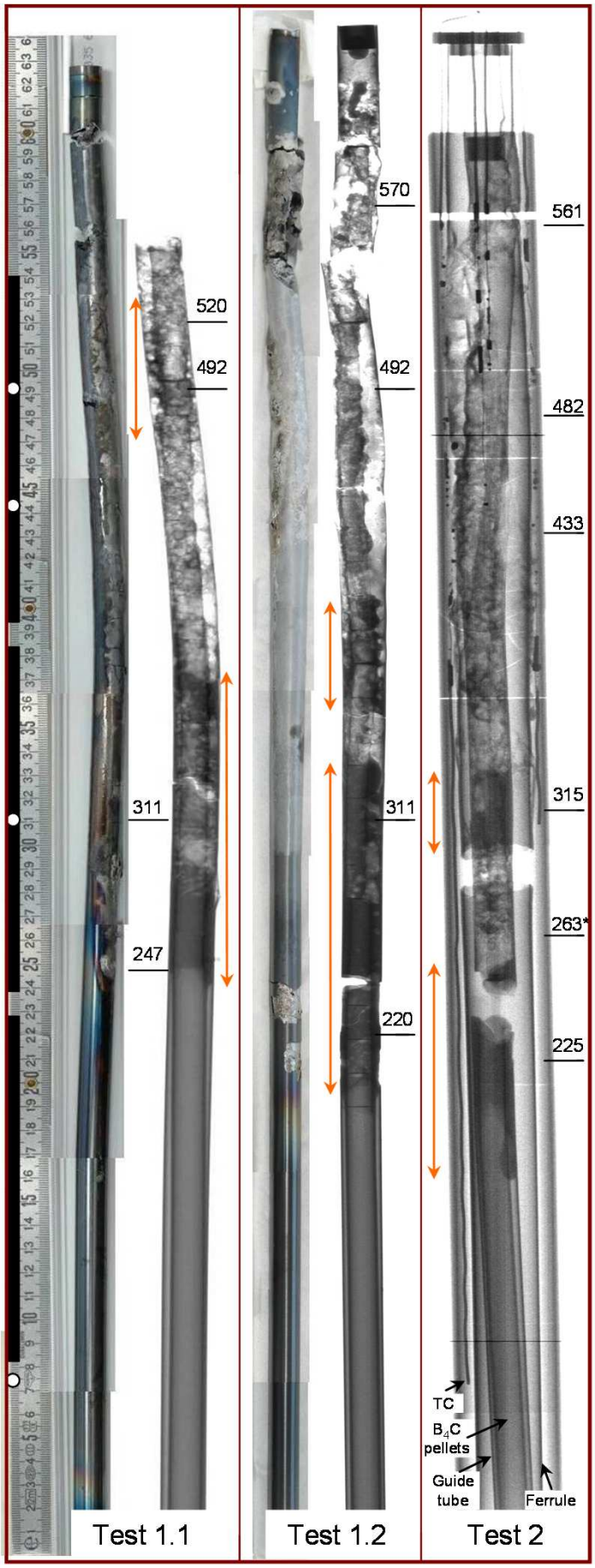

Figure 4: Rod macrographies and radiographies performed after the tests. Orange arrows indicate regions of relocalised metallic mixtures.

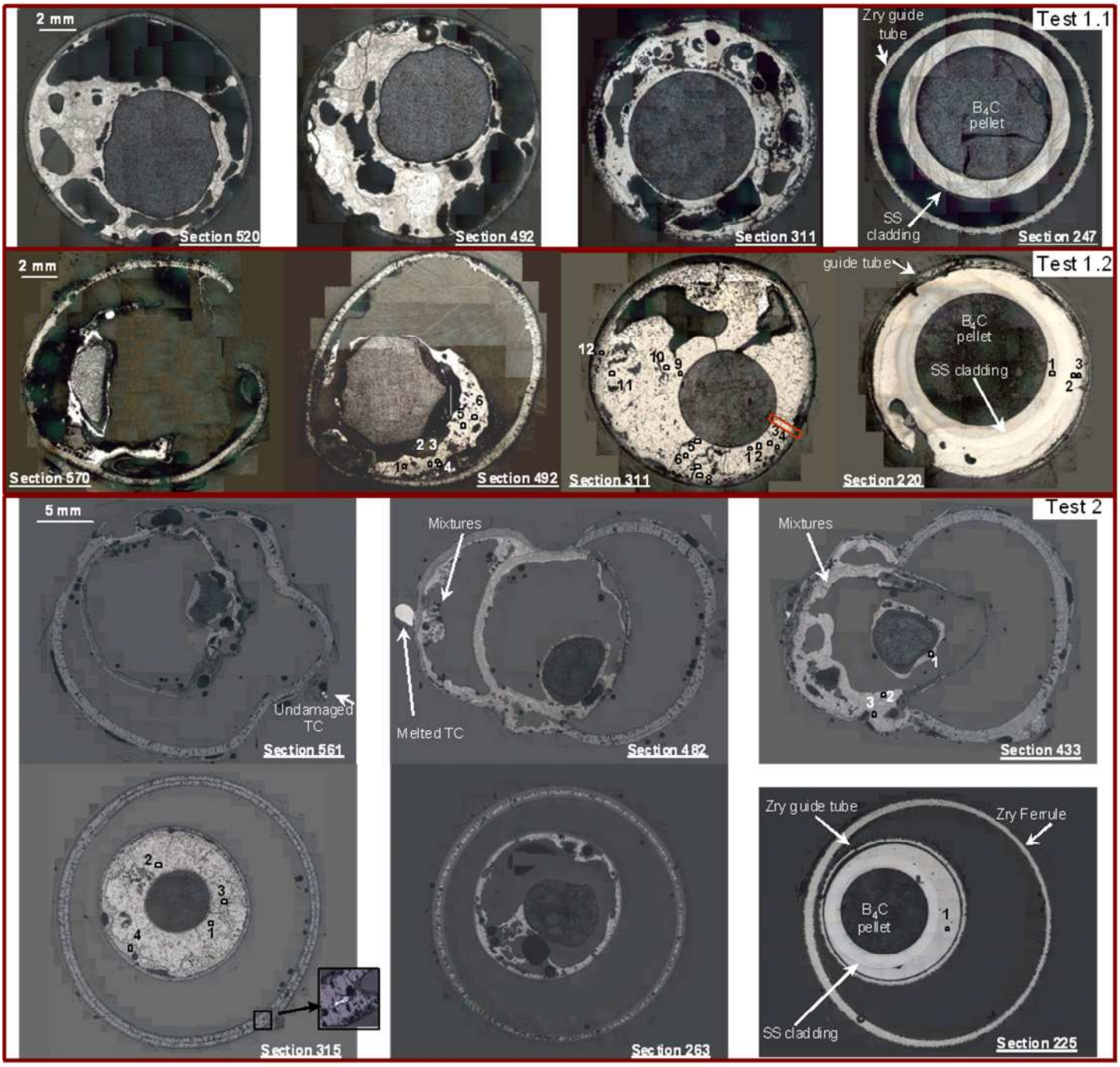

Figure 5: Radial sections of resin embedded specimens. Due to specimen fracture, ferrule observed in section 263 was during the test at level 279 (see explanations in the text).

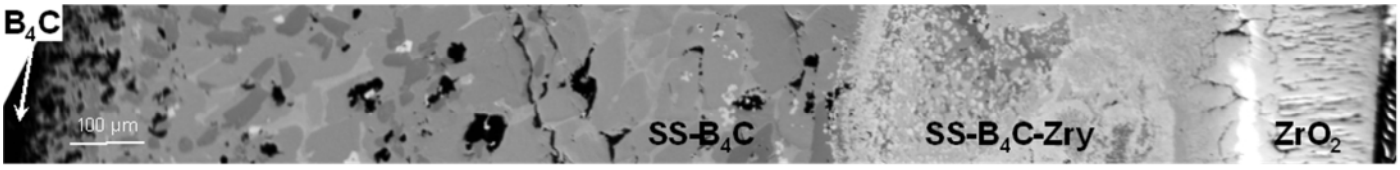

Figure 6: Microstructure of the metallic melt located at section 311 in rod 1.2 (red rectangle in figure 5).

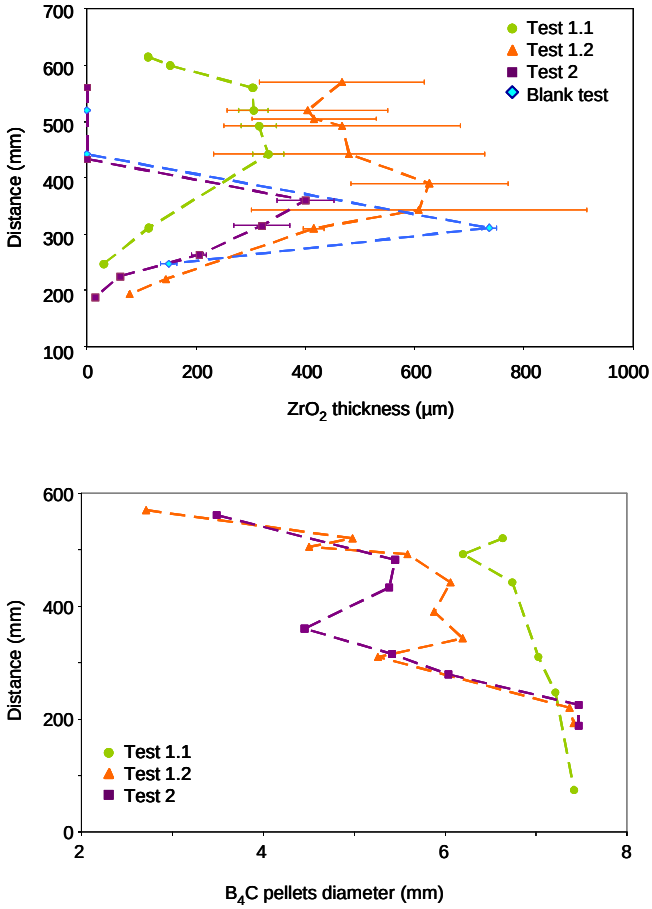

Figure 7 : Thickness of the ZrO_2 scale formed on the guide tube and diameter of B_4C pellets as a function of the distance to the bottom of the control rod.

Test	T_1	t_{stab}	t_{preox}	T_2	t_2
1	1000	0	2000	1680/1340	905
1.2	900	300	2000	1780/1580	2727
2	1000	1871	2580	1780/1580	464
Blank	1000	1407	2580	1780/1580	419

Table 1 : Test parameters. T_1-upper and intermediate resistor temperatures during pre-oxidation plateau, t_{stab}, stabilisation time before steam injection at T_1, t_{preox} steam injection duration at T_1, T_2-upper/intermediate resistor temperatures during high temperature plateau, t_2-duration of high temperature plateau. T in °C and t in s

	Test 1	Test 1.2	Test 2	Blank test
Cladding failure (°C)				
T_{492}	1311	1295	1340	n. d.
T_{442}	-	1333	1367	
Guide tube dislocation (°C)				
T_{492}		1655	1491	
T_{442}	n. d.	1657	1558	n. d.
T_{311}		1474	1546	
T at $H_{2,max}$ (°C)				
$T_{upper\ R}$	1686	1789	1787	1787
T_{492}	1492	1636	1539	1598
T_{442}	-	1661	1628	1646
T_{311}	1235	1429	1802	1643
T_{74}	570	700	-	781
End of degradation (°C)				
T_{492}	1584	1657	-	-
T_{442}	-	1658	-	-
T_{311}	1281	1484	-	-
T_{74}	594	874	-	-
$H_{2,max}$ (mol/min)	0.025	0.056	0.25	0.27
Total quantity (mol)				
H_2	0.35	0.98	2.15	2.65
CO	n. d.	0.023	0.088	n. d.
CO_2	n. d.	0.028	0.002	n. d.
H_2-B_4C oxidation (mol)	-	0.39	0.63	-

n.d- not detected

— - not measured

Table 2: Main temperatures and gases production during the tests.

	B	C	Cr	Fe	Ni	Zr
Test n°1.2						
Section 492						
B_4C-SS-Zry:						
1	19 ± 2	3 ± 1	12 ± 2	40 ± 10	6 ± 2	24 ± 11
2	20 ± 3	5 ± 7	8 ± 3	20 ± 9	3 ± 2	48 ± 16
3	18± 6	7 ± 8	17 ± 8	39 ± 11	3 ± 2	22 ± 18
4	20 ± 4	6 ± 4	12 ± 9	30 ± 17	3 ± 2	38 ± 27
5	20 ± 4	4 ± 4	7 ± 5	34 ± 16	6 ± 1	36 ± 23
6	20 ± 2	4 ± 4	2 ± 2	11 ± 11	3 ± 1	69 ± 15
Section 310						
B_4C-SS:						
1	9 ± 1	10 ± 11	19 ± 5	57 ± 8	6 ± 2	1 ± 2
2	9 ± 2	9 ± 10	19 ± 5	58 ± 6	7 ± 3	1 ± 2
3	8 ± 2	8 ± 9	17 ± 5	59 ± 5	7 ± 4	1 ± 3
5	9 ± 2	7 ± 9	18 ± 7	56 ± 7	8 ± 4	1 ± 1
6	9 ± 2	6 ± 9	16 ± 5	56 ± 5	8 ± 3	1 ± 1
7	8 ± 3	6 ± 7	16 ± 7	56 ± 5	10 ± 5	1 ± 2
9	9 ± 2	10 ± 11	19 ± 6	56 ± 8	6 ± 3	1 ± 2
10	7 ± 2	5 ± 5	13 ± 3	64 ± 3	9 ± 3	0 ± 1
11	6 ± 2	5 ± 2	14 ± 4	63 ± 3	9 ± 4	1 ± 3
B_4C-SS-Zry:						
4	6 ± 6	12 ± 3	5 ± 3	18 ± 10	3 ± 2	64 ± 13
8	7 ± 6	9 ± 4	6 ± 5	21 ± 17	3 ± 2	59 ± 23
12	8 ± 6	9 ± 2	6 ± 4	17 ± 12	3 ± 2	64 ± 16
Section 220						
B_4C-SS: 1	3 ± 1	2 ± 0	18 ± 2	63 ± 2	9 ± 1	0 ± 1
B_4C-SS-Zry:						
2	3 ± 4	2 ± 1	28 ± 4	57 ± 5	4 ± 1	11 ± 8
3	8 ± 4	2 ± 0	15 ± 2	49 ± 4	5 ± 1	28 ± 5
Test n°2						
Section 433						
B_4C-SS-Zry:						
1	17 ± 4	2 ± 1	17 ± 6	52 ± 19	5 ± 4	9 ± 16
2	18 ± 4	3 ± 1	13 ± 6	39 ± 9	5 ± 2	30 ± 12
3	13 ± 5	6 ± 2	4 ± 4	21 ± 14	5 ± 3	56 ± 20
Section 315						
B_4C-SS: 1	10 ± 2	6 ± 9	15 ± 8	59 ± 9	9 ± 5	3 ± 4
2	8 ± 3	3 ± 4	9 ± 6	56 ± 8	17 ± 11	2 ± 3
B_4C-SS-Zry:						
3	10 ± 6	7 ± 4	9 ± 4	27 ± 9	4 ± 1	41 ± 11
4	14 ± 3	6 ± 1	8 ± 4	28 ± 6	4 ± 1	44 ± 8
Section 225						
B_4C-SS: 1	2 ± 1	2 ± 0	27 ± 3	67 ± 2	10 ± 1	0 ± 0

Table 3: Metallic mixtures composition (wt.%) at selected sections of rods n°1.2 and 2.